JP1.10 **INVESTIGATION ON THE CIRCULATION OF URBAN BOUNDARY LAYER INDUCED BY URBANIZED LAND SURFACE**

Soohyun Park, Baek-Min Kim, Gyu-Ho Lim*

School of Earth and Environmental Sciences, Seoul National University, Seoul, South Korea

1. INTRODUCTION

According to the population statistics of resident registration in Seoul, as of late 2004, 0.11% in the total population of Seoul has increased. Also, the area of the city is getting larger every year (Sakong 2002). The urbanization and accompanying concentration of heat distribution nearby urban area are becoming important issue in its own right and also becoming important for understanding global warming trend. The physical processes in urban boundary layer (UBL) of the city have been largely influenced by the characteristic of urbanization. The impact of urbanization on the circulation within UBL can be examined by numerical simulations that utilize different land-use type. The change of land-use type influences on the physical processes of UBL such as net radiation, latent heat flux, sensible heat flux, and ground heat flux (Menglin et al. 2005). The magnitude of the roughness length represents the intensity of mechanical turbulence and other flux quantities above the surface. Henceforth, the enhanced surface turbulence affects heat flux in UBL. The roughness length depends on the frontal area of the average prominences (facing the wind) divided by the ground width it occupies (Wieringa (1998), Henderson-Sellers et. al. (1993)). Huff and Vogel (1978) found that the urban circulation is primarily enhanced by the increase of sensible heat flux and the surface roughness length of the urban area. Hjemfelt (1982) suggested that urban heat intensity increases urban surface roughness, or urban boundary layer instability enhanced convection. The convection enhanced convergence due to the increase of surface roughness in the urban environment (Changnon et al. (1981), Bornstein et. al. (2000), Thielen et al. (2000)).

In this study, we investigate the relationship between physical parameters, such as albedo, moisture variable, emissivity, and roughness length, and atmospheric circulation within UBL in terms of urban canopy dynamics and physics.

2. DATA AND METHOD

2.1. *Data*

* Corresponding author: G.-H. Lim, School of Earth and Environmental Sciences, Seoul National University, Mail Code NS80, Seoul, 151-747, Korea
E-mail: gyuholim@snu.ac.kr

In this research, we used land-use data which is the global data produced by United States Geological Survey (USGS). The global land-use/cover database is classified according to the 25-category USGS land cover system (Anderson et al. 1976). Vegetation cover in the global database was obtained from 1 km Advanced Very High Resolution Radiometer (AVHRR) data spanning from April 1992 through March 1993 but urban areas were added to the dataset after being extracted from the development of the digital chart of the world, which were based on photogram metric analyses of U.S. Department of Defense Corona imagery acquired in the 1960s. Because of this reason, the urban area in this data is not exact. Seo et. al. (2002) produced more accurate land-use data over South Korea from Pathfinder AVHRR for Land (PAL) 1km resolution data. Figure 1 shows the land-use type of AVHRR and PAL over Seoul and its environs of South Korea. Due to the urbanization constantly progressed on since 1960s. the land-use type of the south of Han River (A river crossing from west to east over the central urbanized area in Figure 1) significantly changed.

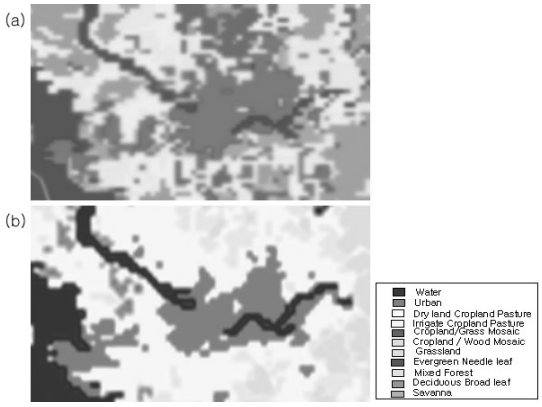

Fig. 1. Land-use type of (a) AVHRR (about 0.9km resolution) and (b) PAL (1km resolution) over Seoul and its environs.

2.2. *Methods*

We focus on the characteristics of near the surface temperature and wind fields in UBL. The near surface temperature is affected by ground temperature, which is affected by sensible heat flux, and latent heat flux and wind profiles. The ground temperature can be decided by surface energy balance equation

$$C_g \frac{\partial T_g}{\partial t} = R_n - SH - LE - G \qquad (1)$$

where C_g is surface heat capacity [$JKg^{-1}K^{-1}$], R_n is the net radiation flux. The net radiation flux is calculated from

$$R_n = (1-\alpha)S_{\downarrow} + LW_{\downarrow} - \varepsilon\sigma T_g^4 \qquad (2)$$

where α is albedo, $S_{\downarrow}$ is downward solar radiation [Wm^{-2}], $LW_{\downarrow}$ is downward long-wave radiation toward the surface layer [Wm^{-2}], ε is emissivity, σ is Stefan-Boltzmann [$Wm^{-2}K^{-4}$], T_g is ground temperature [K], The sensible heat flux SH between the land surface and the atmosphere is calculated from

$$SH = \rho_a c_p C_\theta C_u (\theta_g - \theta_a) V \qquad (3)$$

where ρ_a is air density [Kgm^{-3}], c_p is the heat capacity of air [$JKg^{-1}K^{-1}$], is the turbulent exchange coefficients for heat, C_u is the turbulent exchange coefficient for momentum, θ_g is the potential temperature of the first soil layer [K], θ_a is the lowest prognostic level [K]. The

latent heat flux formula is

$$LE = \lambda \rho_a C_\theta C_u M [q_s(T_g) - q_{va}] V \quad (4)$$

where λ is the latent heat of moisture vapor [JKg^{-1}], M is moisture availability factor, $q_s(T_g)$ is the saturation mixing ratio at T_g, q_{va} is the mixing ratio of water vapor at the lowest prognostic level z_a, V is define by $V = (V_a^2 + V_c^2)^{0.5}$, V_a is the wind speed at the lowest model layer [ms^{-1}], V_c is the convective velocity [ms^{-1}]. The ground heat flux is

$$G = \lambda (T_0 - T_{-1}) / \Delta Z \quad (5)$$

where λ is the thermal conductivity of the substrate and T_{-1} the temperature of the first substrate level, a distance ΔZ below the ground surface, and T_0 is a saturated surface temperature (Grell et al. 1995). The temperature at height of 2 m T_{2m}, and the horizontal components of wind speed at 10 m u_{10m} [ms^{-1}] and v_{10m} [ms^{-1}], are determined diagnostically from the simulated T_g, the air temperature T at the lowest prognostic level z_a, as well as the horizontal wind speed components u [ms^{-1}] and v [ms^{-1}] at z_a, by means of the Monin-Obukhov similarity theory under consideration of the atmospheric stability. The temperature at 2 m and wind speed at 10 m calculate for

$$T_{2m} = T_g + [T_g - T(z_a)] \times \Phi_T(2m) / \Phi_T(z_a) \quad (6)$$

$$u_{10m} = u(z_a) \times \Phi_m(10m) / \Phi_m(z_a), \quad and$$
$$v_{10m} = v(z_a) \times \Phi_m(10m) / \Phi_m(z_a) \quad (7)$$

where $\Phi_T(-)$ and $\Phi_m(-)$ being height-dependent atmospheric stability functions for heat and momentum transfer.

In this study using these equations we investigate the urban canopy dynamics and physics through the model simulations of land-use type change of surface.

3. EXPERIMENTS DESIGN

The selected case, 23 July 2005, sunny and calm day, is proper to studying of circulation within UBL. Seoul weather station had been recorded that the maximum temperature is about 34℃, the minimum temperature is about 26℃ and wind speed is under 3m/s on this day. In this study, the meso-scale model, MM5V3, is used for experiments.

In this study, we do several experiments for understanding the urban effect on UBL as change of land-use type from grass to urban. In the model physical parameters decide the land-use type. The physical parameters, such as albedo, emissivity, moisture variable, roughness length, and thermal inertia, influence on changing radiation and surface fluxes. The model configurations of control experiments describe in Table 1. Firstly, control run (CTR) was carried out. As mentioned previously, based on PAL, AVHRR has smaller urban area especially for the Seoul area. So the urban area was expanded by comparing the urban area of PAL. This experiment is named urban (UB). The land-use type of the urban area of Seoul and Incheon in UB is replaced with grass land-use because almost of grass area is changed with urban area in Figure 1. This experiment is called non-urban (NU). Land-use data of CTR, UB, and NU are shown in Figure 2. Secondly, each physical parameters, albedo (AD, 19% to 15%),

moisture availability (MA, 15% to 10%), emssivity (ES, 98.5% to 88%), roughness length (RA, 12cm to 80cm), are changed from the values of grass land-use type to values of urban land-use type. These experiments are executed to know which the most importance physical parameters effect on the UBL as urbanization occurs.

To interpret the results obtained from the experiment CTR, UB, and NU, we designed idealized experiment exploiting the simplication achieved by flat terrain, fixed lateral boundary condition and constant incoming short wave radiation by fixing the solar insolation during the entire model integration. The short wave radiation was fixed as noon condition. The model configurations of control ideal experiments identify

Table 1. The model configuration of the experiments.

	Domain1	Domain2	Domain3
Gird distance	27km	9km	3km
Grid number	40X39	55X58	52X55
Terrain data	30s	30s	30s
Time step	90s	30s	10s
Moisture scheme	Simple ice	Simple ice	Simple ice
Cumulus scheme	Grell	None	None
Boundary layer	MRF	MRF	MRF
Radiation scheme	CCM2	CCM2	CCM2
Soil	5-layer	5-layer	5-layer
Data	FNL	FNL	FNL
Integrated time	072112-072312	072118-072312	072200-072312

Table 2. The model configuration of the ideal experiments.

	Domain 1
Grid distance	6km
Grid distance	20X36
Moisture scheme	Simple ice
Cumulus scheme	Grell
Boundary layer	MRF
Radiation scheme	CCM2
Soil	5-layer
Data	FNL

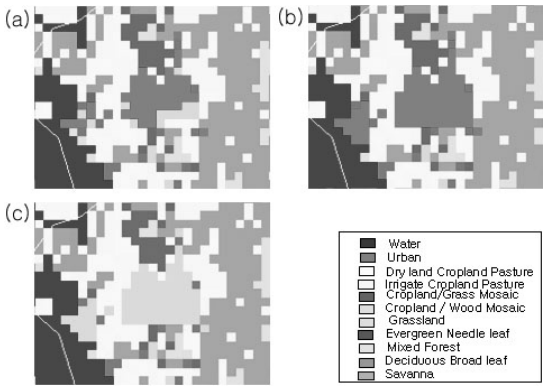

Fig. 2. The modified land-use data (3km resolution) for the domain 3 of (a) CTR, (b) UB, and (c) NU.

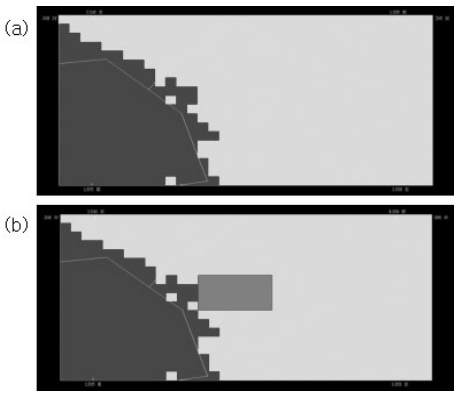

Fig. 3. IGR (a) has only grass land-use type and IUB (b) has grass and urban types. The rectangle area denotes urban area in IUB.

with Table 2. There are two types of land-use, urban (IUB), and grass (IGR) in the ideal experiments (Figure 3). For the sensitivity to roughness length, at idealization condition, values of roughness length of GR was exchanged from 12cm to 25cm (IR_25), to 50cm (IR_50), to 100cm (IR_100), and to 200cm (IR_200) as the classification of Davenport-Wieringa roughness length.

4. RESULTS

The urban area mean potential temperature of

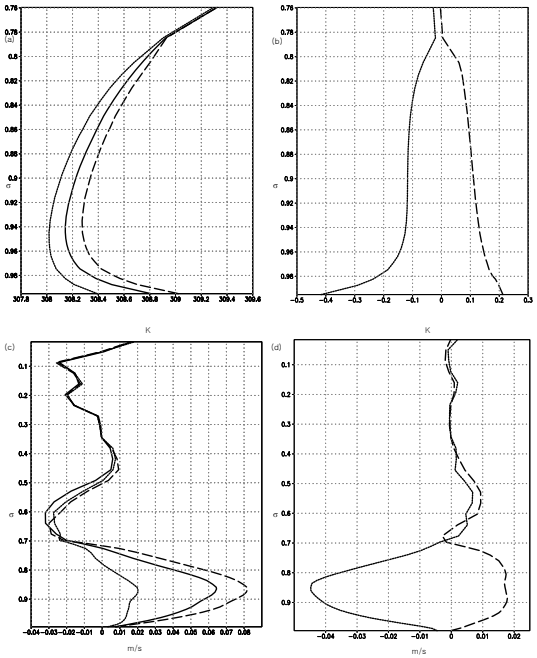

Fig. 4. The urban area mean profiles of potential temperature and the maximum vertical velocity profiles. (a) and (c) are for CTR (solid), UB (long dash), NU (short dash). (b) and (d) are the profiles for UB-CTR (long dash) and NU-CTR (short dash).

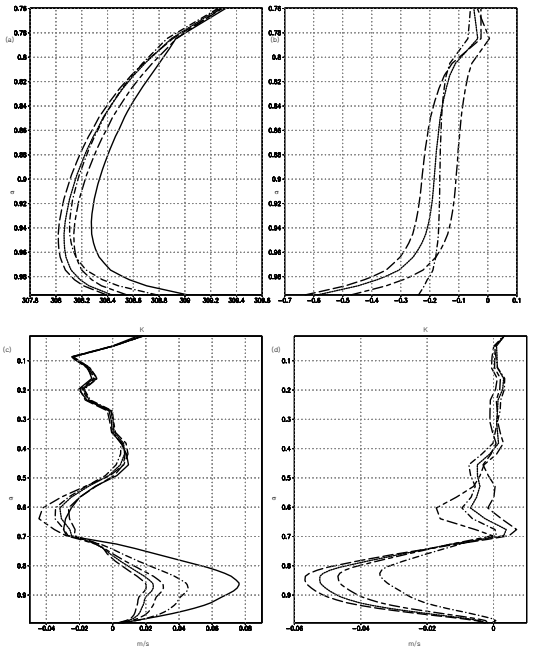

Fig. 5. The profiles of area mean potential temperature and the maximum vertical velocity profiles (a) and (c) are for AD (dot dash), MA (long short dash), EM (long dash), RL (long dot dash), and UB (solid). (b) and (d) are for AD-UB (dot dash), MA-UB (long short dash), EM-UB (long dash), and RL-UB (long dot dash).

UB is 0.6℃ warmer than NU near surface (Figure 4 (a), (b)). Comparing of slant of potential temperature profiles near the surface, UB is the most unstable in UBL. The vertical velocity profiles mean at the maximum vertical velocity station, which locates downwind side in urban area. The maximum difference of vertical velocity within UBL is 0.07m/s when land-use type is exchanged from grass to urban (Figure 4 (c), (d)). The tilt of RL profile is similar to tilt of UB profile near surface (Figure 5. (a), (b)). The roughness length affects the static stability of atmospheric near the surface.

The vertical velocity profile of RL is the nearest structure with vertical velocity profile of UB (Figure 5. (c), (d)). Roughness length has effect vertical velocity on whole UBL. Through these results, among the physical parameters, roughness length is the most effect vertical velocity and potential temperature within UBL.

In ideal experiments, when urban exists, value of urban area mean potential temperature of IUB is 0.5℃ warmer near surface than IGR and value of the maximum vertical velocity of IUB is 0.06m/s faster than IGR within UBL (Figure 6). The potential temperature sensitively reacts near surface in UBL as chang to urban land-use type, but the vertical velocity is affected on entire UBL as change to urban land-use type. The urban land-use type has different values of physical parameters compare with values of physical parameters grass land-use type. According to pre-results roughness length plays an important role on urban effect. Figure 7 is the results of sensitivity for roughness length. Near surface, the slope of potential temperature profiles is more tilt when roughness length is longer (Figure 7. (a), (b)). We can have the static stability values like as -4.04K/km, -4.5K/km, -5.6K/km, and -7.6K/km, as

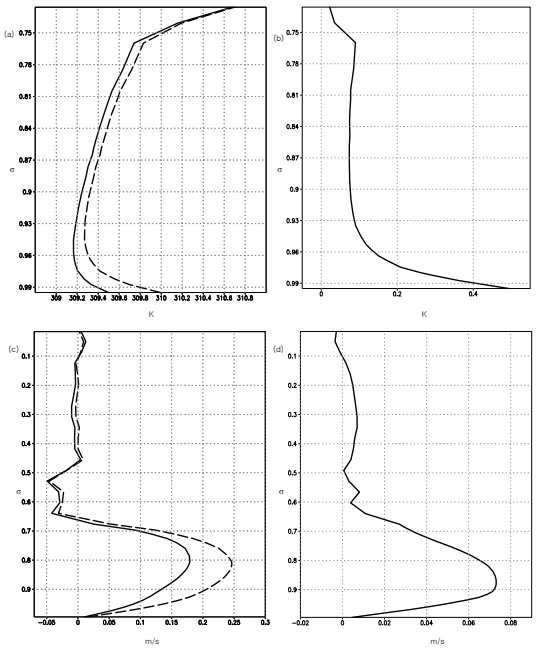

Fig. 6. The profiles of area mean potential temperature and the maximum vertical velocity profiles (a) and (c) are for IUB (long dash), IGR (solid). (b) and (d) are for IUB-IGR (solid).

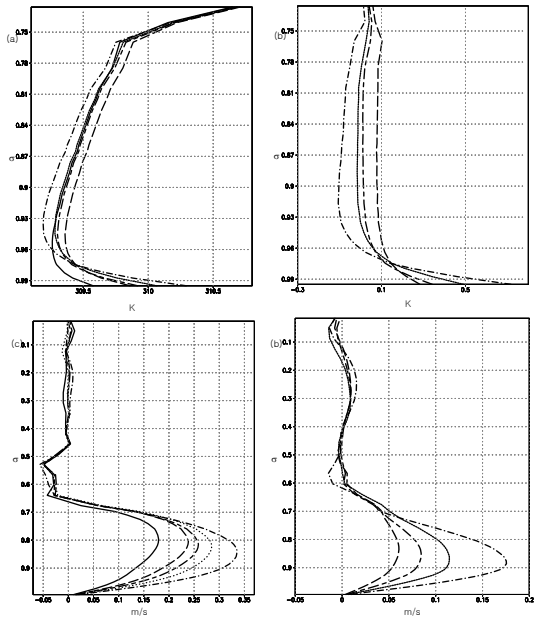

Fig. 7. The profiles of area mean potential temperature and the maximum vertical velocity profiles (a) and (c) are for IGR(solid), IR25 (long dash), IR50 (long short dash), IR100 (dot dash), and IR200 (long dot dash) (b) and (d) are for IR25-IGR (long dash), IR50-IGR (long short dash), IR100-IGR (dat dash), and IR200-IGR (long dot dash).

IR25, IR50, IR100, and IR200. That is, the value of roughness length is larger, value of static stability is smaller near surface. The reason of these results is that the instability functions in (6) and (7) are affected by roughness length. Also the vertical velocity within UBL is faster as the value of roughness length increase (Figure 7. (c), (d)). The near surface potential temperature and vertical velocity in UBL are the most sensitive with roughness length in particular.

5. SUMMARY

In MM5, typical are characterized by albedo (15%), moisture availability (10%), emissivity (88% at 9 m), roughness length (80cm), and thermal inertia (0.03 cal cm^{-2} k^{-1} $s^{-1/2}$) which are specified in land use type. Modifying the values specified in land use type carefully, we could examine the sensitivity of meteorological variables on the change of urban surface properties. Windless and sunny day over Korean peninsula in summer (July 23, 2005) was selected as initial condition. With this model setup, surface energy balance equation which is directly related with the temperature and wind within UBL was examined in detail. As the land-use type changes from grass to urban, mean potential temperature of near-surface becomes 0.5℃~0.6℃ warmer and vertical velocity, usually observed over the downwind side in urban area, becomes the maximum 0.06m/s~0.07m/s stronger within UBL. Among physical parameters characterizing urban surface, roughness length was found to be most influencing factor for the near surface potential temperature and wind within UBL. It was found that the roughness length is tightly related to static stability near sub-UBL. As roughness length increases (25cm, 50cm, 100cm and 200cm), the static stability values within sub-UBL increased -4.0K/km, -4.5K/km, -5.6K/km, and -7.6K/km in ideal experiments. Related to this, the vertical motion was enhanced within the UBL. These results are consistent with other studies such as Bornstein et. al (2000), Thielen et. al. (2000).

Reference

Suh, M.-S., Suh, A.-S., 2003: Characteristics of PAL of East Asia and 3-d Check Noises and Correction Techniques, *J. of the Korean Meteor. Soc.*, 39, 139-150.

Sakong, H.-S., 2002: Study about Characteristics and Diffusion process of Seoul using GIS and Remote sensing, A doctor thesis of University of Seoul, 150 pp.

Anderson, J. R., E. E. Hardy, j. T. Roach, and R. E. Witmer, 1976: A land-use and land cover classification system for use with remote sensor data. U.S. Government Printing Office, Paper 964, 28pp.

Bornstein, R., and Q. Lin, 2000: Urban heat islands and summertime convective thunderstorms in Atlanta: Three cases studies. *Atmos. Environ.*, 34, 507-516.

Changnon, S. A., R. G. Semonin, A. H. Auer, R. R. Braham, and J. Hales, 1981: *METROMEX: A Review and Summary.*

Meteor. Monogr., No. 40, Amer. Meteor., No. 40, Amer. Meteor. Soc., 81pp.

Grell, A. G., and J. dudhia, and D. R. Stauffer, 1995: A description of the fifth-generation Penn State/NCAR Nesoscale Model (MM5). NCAR Tech. Note NCAR/TN-298+STR, 122 pp.

Henderson-Sellers, A., Dickinson, R.E., Durbidge, T.B., Kennedy, P.J., McGuffie, K. and Pitman, A.J., 1993. Tropical deforestation: modelling local to regional-scale climate change, *Journal of Geophysical Research*, 98(D4),

Hjemfelt, M. R., 1982: Numerical simulation of the effects of St. Louis on mesoscale boundary layer airflow and vertical motion: Simulations of urban vs. non-urban effects. *J. Appl. Meteor.*, 21, 1239-1257.

Huff F. A., and J. L. Vogel, 1978: Urban, topographic and diurnal effects on rainfall in the St. Louis region. *J. Appl. Meteor.,* 17, 565-577

J., Menglin, and Shepherd M. 2005: Inclusion of urban landscape in a climate model: How can satellite data help?, *Bull. Amer. Meteo. Soc.*, 86, 681-689.

Thielen, J., W. Wobrock, A. Gadian, P. G. Mestayer, and J.-D. Creutin, 2000: The possible influence of urban surfaces on rainfall development: A sensitivity study in 2D in the meso-gamma scale. *Atmos. Res.,* 54, 15-39

Wieringa, J. 1998. How far can agro meteorological station observations be considered representative? Preprint to 23rd *Amer. Meteor. Soc.* Conference on Agric. and Forest Meteor. (Albuquerque).